Journal of Earthquake Engineering

ISSN: (Print) (Online) Journal homepage: https://www.tandfonline.com/loi/ueqe20

An Efficient Method for Probability Prediction of Peak Ground Acceleration Using Fourier Amplitude Spectral Model

Rui Zhang, Yan-Gang Zhao & Haizhong Zhang

To cite this article: Rui Zhang, Yan-Gang Zhao & Haizhong Zhang (2023): An Efficient Method for Probability Prediction of Peak Ground Acceleration Using Fourier Amplitude Spectral Model, Journal of Earthquake Engineering, DOI: 10.1080/13632469.2023.2241549

To link to this article: https://doi.org/10.1080/13632469.2023.2241549

Published online: 09 Aug 2023.

JOURNAL OF EARTHQUAKE ENGINEERING
https://doi.org/10.1080/13632469.2023.2241549

An Efficient Method for Probability Prediction of Peak Ground Acceleration Using Fourier Amplitude Spectral Model

Rui Zhang[a], Yan-Gang Zhao[a], and Haizhong Zhang[b]

[a]Key Laboratory of Urban Security and Disaster Engineering of Ministry of Education, Beijing University of Technology, Beijing, China; [b]Eco-Science Course, Faculty of Agriculture, Yamagata University, Tsuruoka-Shi, Yamagata, Japan

ABSTRACT
The probabilistic prediction of peak ground acceleration (PGA) using the Fourier amplitude spectral (FAS) model has many advantages in regions lacking strong ground-motion records. Currently, the implementation of this approach for the calculation of annual exceedance rate of PGA relies on Monte Carlo simulations (MCSs). However, adopting MCS requires many times calculations of PGA from FAS, and each time of calculation includes complicated integrals, the computational cost is too high to be acceptable for practical applications. Therefore, this study proposes an efficient method for the probabilistic prediction of PGA using the FAS model. For this purpose, a probabilistic analysis method, referred to as the moment method, was introduced to improve computational efficiency. The probability distribution of PGA was approximated using a three-parameter distribution defined according to the first three moments. The first three moments of the PGA were obtained based on the point-estimate and dimension-reduction integration method. Numerical examples were conducted to verify the proposed method. It was found that the proposed method not only performed much more efficiently than using MCS in calculating the annual exceedance rate of PGA to obtain the hazard curve but also provides nearly the same accuracy as MCS.

ARTICLE HISTORY
Received 10 April 2023
Accepted 22 July 2023

KEYWORDS
Peak ground acceleration; Fourier amplitude spectral model; moment method; point-estimate method; dimension-reduction integration

1. Introduction

Probabilistic seismic hazard analysis (PSHA) is an important tool for providing seismic hazard information for regional planning, important project plans such as nuclear power plants and dams (Jarahi 2017; Villani et al. 2020), and common structural designs (Eurocode 8 2004; Fujiwara et al. 2006; GB 18306 2015). The main objective of the PSHA is to estimate the ground-motion intensity in a probabilistic manner and to obtain exceedance probabilities corresponding to different levels of intensity values. The PSHA has adopted many hazard measures, such as peak values of ground motion and response spectra at representative periods. Of which peak ground acceleration (PGA) is still one of the most widely used hazard measures owing to its simplicity, and its results from PSHA are often used coupling with spectral shape models related to site conditions, distance, etc., to construct design response spectra (Drouet et al. 2020; Du and Pan 2020; Eurocode 8 2004; Falak et al. 2023; Foytong et al. 2020; GB 18306 2015; GB 50011–2010 2016; Hsu et al. 2020; JGJ 3–2010; Li et al. 2020; Mahmoud, Mohamed, and Hanan 2021; Rahman et al. 2021; RLB 2015; Saurav et al. 2022; Sinhal and Sarkar 2020). Therefore, the probabilistic prediction of PGA has received considerable attention. The basic steps of the probabilistic prediction of PGA involve the following: (1) identification of potential seismic sources and their recurrences, (2) determination of the probability distribution of the main seismic parameters, for example, magnitude and distance, (3)

CONTACT Haizhong Zhang zhang@tds1.tr.yamagata-u.ac.jp Eco-Science Course, Faculty of Agriculture, Yamagata University, 1-23, Wakaba-machi, Tsuruoka-shi, Yamagata 997-8555, Japan

selection of reasonable ground-motion prediction equations (GMPEs) for PGA, and (4) calculation of the exceedance probability of the PGA. It is known that, a GMPE for PGA is necessary for the probabilistic prediction of PGA. In the past several decades, numerous studies have focused on the development of GMPEs for PGA (Douglas 2021), and many equations have been constructed based on the regression of ground-motion records. However, most of these GMPEs were developed for regions with rich earthquake data, and there are almost no GMPEs for regions lacking earthquake data owing to insufficient data required for regression. In addition, because of the different seismological characteristics in different regions, GMPEs from regions with rich earthquake data may not be available for regions lacking earthquake data. Therefore, it is difficult to perform probabilistic predictions of PGA in regions lacking strong ground records using the traditional procedure.

Many studies (Atkinson 2008; Atkinson and Boore 2006; Bora et al. 2014, 2016; Campbell 2003; Cotton et al. 2006) have been devoted to solving the problem of probabilistic prediction of PGA in regions lacking strong ground-motion records. Cotton et al. (2006) weighted averaged several GMPEs from data-rich regions to approximate a GMPE for use in regions lacking strong ground records. Considering the subjectivity of the selection as well as regional differences in the GMPEs when adopting the approaches of Cotton et al. (2006), Campbell (2003) and Atkinson (2008) suggested adjusting an GMPE in data-rich to data-poor regions using the PGA ratios in the two regions. Bora et al. (2014) pointed out that because the scaling of PGA from the source to the site is inconsistent with the linear system theory, PGA ratios do not purely reflect the differences between the two regions. Therefore, Bora et al. (2014, 2016) suggested using the GMPE of the Fourier amplitude spectrum (FAS) to simulate ground motion and then estimated the PGA based on the random vibration theory (RVT). FAS corresponds to the linear system theory and is more suitable for adjustment. Similarly, Boore (2003) used a FAS model, expressed in terms of various sources, paths, and site parameters, to characterize ground motion. The advantage of using the FAS model is that it can be determined using limited earthquake data with small-to-moderate magnitudes in regions lacking ground-motion records. The method of Boore (2003) has been adopted by many studies (Atkinson and Boore 2006; Boore 2018, 2020; Bora et al. 2016; Hassani and Atkinson 2015) to develop GMPEs in regions lacking strong ground motion records. In contrast to these studies, Zhao, Zhang, and Zhang (2023) directly used the FAS model, instead of developing a GMPE using the stochastic method, to conduct probabilistic prediction of PGA. Zhao, Zhang, and Zhang (2023) calculated the PGA from ground-motion FAS based on RVT according to Boore (2003). Then, they obtained hazard curves of PGA considering uncertainties of various seismological parameters, such as magnitude, distance, and stress drop, as well as all potential seismic sources using a Monte Carlo simulation (MCS). The method proposed by Zhao, Zhang, and Zhang (2023) avoids the process of developing a GMPE based on stochastic simulation as well as the additional uncertainties caused by this process. However, when applying MCS to address uncertainties of the seismological parameters, such as magnitude, distance, and stress drop, etc., to obtain the exceedance probability of PGA, many times calculations of PGA from FAS (equaling the product of the sample number of MCS and the number of seismic sources) need to be repeated. In addition, the calculation of PGA from FAS based on the random vibration theory includes many complex numerical integrations. In particular, when a small exceedance probability is of interest, the sample number of MCS can be considerably large, which makes the calculation time as long as several hours even for simple cases. Hence, the inefficiency of the method of Zhao, Zhang, and Zhang (2023) limits its practical application.

To improve computational efficiency, an efficient method for the probabilistic prediction of PGA based on the FAS model was proposed in this study. The remainder of this paper is organized as follows. First, the method of probabilistic prediction of PGA by Zhao, Zhang, and Zhang (2023) is briefly reviewed in Section 2. In Section 3, a probabilistic analysis method, namely the moment method (Zhao and Lu 2021), is innovatively introduced to improve computational efficiency. In Section 4, the efficiency and accuracy of the proposed method are verified using three examples and compared with the MCS. Finally, the conclusions of this study are summarized in Section 5.

2. Probabilistic Prediction of PGA Using FAS Model Based on MCS

2.1. FAS Model

Zhao, Zhang, and Zhang (2023) adopted a FAS model introduced by Boore (2003). The FAS of ground-motion acceleration at the surface, $Y(f)$, is expressed as an explicit function of the source term, $E(M_0, f)$, propagation path term, $P(R, f)$, and site term, $G(f)$,

$$Y(f) = E(M_0,f)P(R,f)G(f) \tag{1}$$

where f is the frequency, R is the source-to-site distance, and M_0 is the seismic moment. The seismic moment M_0 can be related to the moment magnitude M by $M_0 = 10^{1.5M + 16.05}$ (Hanks and Kanamori 1979).

The source term $E(M_0, f)$ is commonly expressed by the Brune ω-squared point-source spectrum, although many other source spectrum models are equally valid (Boore 2003). Substituting the ω-squared point source spectrum and expressions for the path and site terms into Eq. (1) yields (Boore 2003)

$$Y(f) = \left[0.78\frac{\pi}{\rho\beta^3}M_0\frac{f^2}{1+\left(\frac{f}{f_c}\right)^2}\right]\left[Z(R)\exp\left(\frac{-\pi fR}{Q(f)\beta}\right)\right][\exp(-\pi\kappa_0 f)A(f)] \tag{2}$$

where ρ is the mass density of the crust, β is the shear-wave velocity of the crust, $Z(R)$ represents the geometric attenuation, $Q(f)$ represents the anelastic attenuation, κ_0 is the diminution parameter, $A(f)$ represents the crust amplification, and f_c is the corner frequency representing the frequency below which the FAS decays $f_c = 4.9 \times 10^6\beta(\Delta\sigma/M_0)^{1/3}$, $\Delta\sigma$ is the stress drop. Researchers have made great efforts for the determination of these seismological parameters. Hanks and McGuire (1981) and Atkinson and Boore (2014) discussed the stress drop $\Delta\sigma$ based on earthquakes in Eastern North America. Folesky, Kummerow, and Shapiro (2021) estimated stress drops $\Delta\sigma$ based on 534 earthquakes in Northern Chile. Nakano and Kawase (2019) calculated stress drop $\Delta\sigma$ based on the 2018 Hokkaido Iburi-Tobu earthquake in Japan. In addition, Boore and Joyner (1997) and Boore and Thompson (2015) studied the crust amplification $A(f)$ in America. Moreover, Atkinson (1996) studied the diminution parameter κ_0 in Eastern and Western Canada. Campbell (2009) studied the diminution parameter κ_0 for unconsolidated and semiconsolidated sediments in Eastern North America. Sun et al. (2013) derived the κ_0 based on the 2008 Wenchuan earthquake in China.

2.2. Estimation of PGA from FAS Based on RVT

Because the RVT can relate the peak value of a time-history motion to the motion's FAS, the PGA can be obtained from the ground-motion FAS based on the RVT, which can be expressed as

$$\mathrm{PGA} = pf\sqrt{\frac{1}{D\pi}\int_0^\infty |Y(\omega)|^2 d\omega} \tag{3}$$

where $Y(\omega)$ is the FAS of the ground motion, ω is the circular frequency, and D is the ground-motion duration related to the corner frequency f_c and distance R, expressed as $D = 1/f_c + 0.05R$ (Atkinson and Silva 2000).

The use of RVT to predict PGA goes back to the 1980s (Boore 1983; Hanks and McGuire 1981; Vanmarcke and Lai 1980). This approach has been verified and widely applied by seismologists and engineers for several decades (Boore 1983; Campbell 2003; Hanks 1979; Hanks and McGuire 1981; Kottke and Rathje 2013; Rathje and Ozbey 2006; Wang and Rathje 2018). Nevertheless, the RVT approach is not perfect due to the assumption of stationarity of strong-ground time histories. To overcome this demerit, the ground motion duration is an essential element of the RVT framework, and Bora et al. (2014, 2015, 2019) and Kolli and Bora (2021) have made great efforts in this aspect.

In Eq. (3), *pf* is the peak factor, which is defined as the ratio of the peak motion to the root-mean-squared motion. Many peak factor models have been developed for RVT analyses (Cartwright and Longuet-Higgins 1956; Davenport 1964; Vanmarcke 1975). Although the Cartwright and Longuet-Higgins model has been commonly applied in engineering seismology and site-response analyses, the Vanmarcke model provides better estimations of the peak factor (Wang and Rathje 2016). The cumulative distribution function (CDF) of the peak factor *pf* provided by Vanmarcke (1975) is expressed as follows:

$$P(pf < r) = \left[1 - \exp\left(-\frac{r^2}{2}\right)\right] \exp\left\{-2f_z \exp\left(-\frac{r^2}{2}\right) D \frac{\left[1 - \exp\left(-\sqrt{\frac{\pi}{2}}\delta^{1.2} r\right)\right]}{1 - \exp\left(\frac{r^2}{2}\right)}\right\} \tag{4}$$

where δ is the bandwidth factor of FAS, which is defined as a function of the spectral moments of FAS as follows.

$$\delta = \sqrt{1 - \frac{(m_1)^2}{m_0 \times m_2}} \tag{5}$$

where m_n ($n = 0, 1, 2$) denotes the nth order spectral moment of the square of FAS, defined by

$$m_n = \frac{1}{\pi} \int_0^{\infty} \omega^n |Y(\omega)|^2 d\omega \tag{6}$$

where f_z is the rate of zero crossing, and it is defined as follows.

$$f_z = \frac{1}{2\pi} \sqrt{\frac{m_2}{m_0}} \tag{7}$$

2.3. Estimating the Exceedance Probability of PGA Using MCS

The exceedance probability of PGA $P(\mathrm{PGA} > pga; t)$, focused on in this study, is defined as the PGA exceeding a specific level *pga* at a specific time interval t (year) considering all potential seismic sources. It can be expressed as follows (Fujiwara et al. 2006)

$$P(\mathrm{PGA} > pga; t) = 1 - \prod_{k=1}^{n_k} [1 - P_k(\mathrm{PGA} > pga; t)] \tag{8}$$

where k refers to the kth earthquake and $P_k(\mathrm{PGA} > pga; t)$ is the probability that PGA exceeds *pga* over time t for the kth earthquake, n_k is the number of seismic sources.

Typically, the occurrence of a seismic event is assumed to follow a Poisson arrival process (Cornell 1968); thus the probability that PGA exceeds a special level *pga* over time t, $P_k(\mathrm{PGA} > pga; t)$, can be expressed as

$$P_k(\mathrm{PGA} > pga; t) = 1 - e^{-p_k v_k t} \tag{9}$$

where v_k is the mean annual rate of the kth earthquake and p_k is the probability that the PGA exceeds *pga* for the occurrence of the kth earthquake. Commonly, m and r are considered random variables, and p_k is expressed as follows (McGuire 1976):

$$p_k(pga) = \int_R \int_M P(\mathrm{PGA} > pga | m, r) f_M(m) f_R(r) dm dr \tag{10}$$

where $P(\mathrm{PGA} > pga|m, r)$ is the conditional probability that PGA is greater than the intensity pga for a given magnitude m and source-to-site distance r, $f_M(m)$ is the probability density function (PDF) of the magnitude, and $f_R(r)$ is the PDF of the source-to-site distance.

The general expression of $p_k(pga)$, considering arbitrary numbers of random variables, is given by

$$p_k(pga) = \int_{X_1} \cdots \int_{X_i} \cdots \int_{X_n} P\left(pf \sqrt{\frac{1}{D\pi} \int_0^{\infty} |Y(\omega)|^2 d\omega} > pga | X_1, \cdots, X_i, \cdots, X_n \right) \times f_{X_1}(x_1) \cdots f_{X_i}(x_i) \cdots f_{X_n}(x_n) dx_1 \cdots dx_i \cdots dx_n \tag{11}$$

where ω is the circular frequency, and $\omega = 2\pi f$; X_i $(i = 1, 2, \cdots, n)$ represent the seismological parameters, such as magnitude M, source-to-site distance R, stress drop $\Delta\sigma$, shear-wave velocity of the crust β, mass density of the crust ρ, diminution parameter κ_0, etc., they are all considered as independent random variables; $f_{Xi}(x_i)$ is the PDF of the random variable X_i, and n is the number of random variables.

Given that Eq. (11) includes a complicated high-dimensionality integral, its analytical solution cannot be obtained. Zhao, Zhang, and Zhang (2023) solved Equation (11) using the MCS. Since the uncertainties of the seismological parameters (such as magnitude and distance) are considered, it is necessary to calculate the PGA from the FAS based on the RVT many times. The detailed calculation steps are shown in Fig. 1.

As shown in Fig. 1, the method of Zhao, Zhang, and Zhang (2023) needs additional calculations of the PGA from the FAS to obtain the exceedance probability of PGA, and the calculation includes numerous complex numerical integrations. In addition, owing to the application of MCS, such calculations of PGA need to be repeated n_m times for a single source, where n_m is the sample number of MCS. When a small exceedance probability is of interest, the sample number of MCS can be

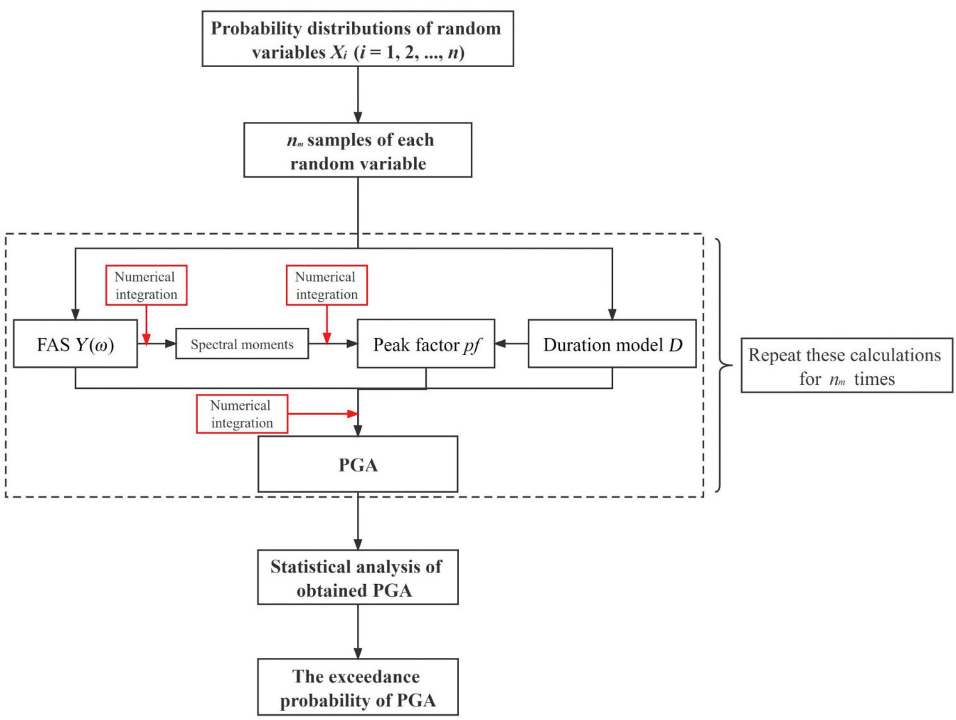

Figure 1. Flowchart of the method by Zhao, Zhang, and Zhang (2023). X_i ($i = 1, 2, \cdots, n$) are random variables representing the magnitude M, source-to-site distance R, stress drop $\Delta\sigma$, the shear-wave velocity of the crust β, mass density of the crust ρ, and diminution parameter κ_0.

considerably large (usually n_m is larger than 10^5), because of which the calculation time is as long as several hours even for simple cases.

Two simple examples of calculating the annual exceedance rate of PGA and the hazard curve considering one and four sources were performed using MCS in our previous study, which cost as long as approximately one hour, considering only 10,000 samples for each random variable (Zhao, Zhang, and Zhang 2023). A larger number of samples is required in MCS when a small exceedance probability is of interest. In addition, there are a lot of earthquake sources that need to be considered in real cases. Therefore, a longer time is required to obtain the exceedance probability of the PGA. To improve the practicability of the method proposed by Zhao, Zhang, and Zhang (2023), it is necessary to improve the efficiency of obtaining the exceedance probability of PGA.

3. Probabilistic Prediction of PGA Using FAS Model Based on the Moment Method

To improve the computational efficiency for calculating the exceedance probability of the PGA, it is necessary to reduce the calculation times of the PGA from FAS based on RVT. To realize this purpose, methods based on probabilistic theory are promising. The moment method using the first few moments and an assumed probability distribution of PGA can solve this problem by performing a few calculations of PGA from FAS based on RVT. The first few moments of PGA can be obtained using the point-estimate method, which requires only a few calculations times of PGA from the FAS based on RVT.

3.1. Probability Distribution of PGA

To simply calculate the exceedance probability of PGA, a CDF of the PGA is assumed. Because of the ability of the three-parameter probability distribution to reflect the skewness characteristics, a three-parameter probability distribution based on the third-moment standardization function (Zhao and Ono 2000b, Zhao et al. 2001) is adopted, which can be expressed as

$$F_{\mathrm{PGA}}[\mathrm{PGA}(X_1,\cdots,X_i,\cdots,X_n)]=\Phi\left[\frac{1}{\alpha_{3\mathrm{PGA}}}\left(\sqrt{9+\frac{1}{2}\alpha_{3\mathrm{PGA}}^2+6\alpha_{3\mathrm{PGA}}\frac{\mathrm{PGA}-\mu_{\mathrm{PGA}}}{\sigma_{\mathrm{PGA}}}}-\sqrt{9-\frac{1}{2}\alpha_{3\mathrm{PGA}}^2}\right)\right] \tag{12}$$

where $\mathrm{PGA}(X_1, \cdots, X_i, \cdots, X_n)$ is a random variable depending on the probability distributions of X_i, μ_{PGA} is the mean of PGA, σ_{PGA} is the standard deviation of PGA, $\alpha_{3\mathrm{PGA}}$ is the skewness of PGA, $\Phi(\cdot)$ is the CDF of a standard normal random variable. It should be noted that Eq. (12) is determined by three parameters, μ_{PGA}, σ_{PGA} and $\alpha_{3\mathrm{PGA}}$, which are the first, second, and third moments, respectively.

The first three moments of the PGA, mean μ_{PGA}, standard deviation σ_{PGA}, and skewness $\alpha_{3\mathrm{PGA}}$ can be estimated as follows:

$$\begin{aligned}\mu_{\mathrm{PGA}}&=\mu_{1\mathrm{PGA}}\\ \sigma_{\mathrm{PGA}}&=\sqrt{\mu_{2\mathrm{PGA}}-\mu_{1\mathrm{PGA}}^2}\\ \alpha_{3\mathrm{PGA}}&=\frac{\mu_{3\mathrm{PGA}}-3\mu_{2\mathrm{PGA}}\mu_{1\mathrm{PGA}}+2\mu_{1\mathrm{PGA}}^3}{\sigma_{\mathrm{PGA}}^3}\end{aligned} \tag{13}$$

where $\mu_{1\mathrm{PGA}}$, $\mu_{2\mathrm{PGA}}$, and $\mu_{3\mathrm{PGA}}$ are the first, second, and third raw moment of PGA, respectively. The kth raw moment of PGA, $\mu_{k\mathrm{PGA}}$ ($k = 1, 2, 3$), can be formulated as

$$\mu_{k\mathrm{PGA}} = E\left\{[\mathrm{PGA}(X_1, \cdots, X_i, \cdots, X_n)]^k\right\} = \underbrace{\int_{-\infty}^{+\infty} \cdots \int_{-\infty}^{+\infty}}_{n} [\mathrm{PGA}(X_1, \cdots, X_i, \cdots, X_n)]^k \times f_{X_1}(x_1) \cdots f_{X_i}(x_i) \cdots f_{X_n}(x_n) dx_1 \cdots dx_i \cdots dx_n \tag{14}$$

where $E\{\cdot\}$ is the expectation operator.

3.2. Calculation of the First Three Raw Moments of PGA

Similar to Eq. (11), the analytical solution for $\mu_{k\mathrm{PGA}}$ in Eq. (14) cannot be obtained owing to the complicated high-dimensionality integral. Because the MCS requires too many function calls of [PGA $(X_1, \cdots, X_i, \cdots, X_n)]^k$ to estimate Eq. (14), the point-estimate method was adopted to calculate $\mu_{k\mathrm{PGA}}$ (Rosenblueth 1975). The point-estimate method uses a weighted sum of the results of $[\mathrm{PGA}(X_1, \cdots, X_i, \cdots, X_n)]^k$ evaluated at a finite number of points to approximate $\mu_{k\mathrm{PGA}}$ and only requires a few function calls of $[\mathrm{PGA}(X_1, \cdots, X_i, \cdots, X_n)]^k$. Based on the point-estimate method, the kth raw moments of PGA $\mu_{k\mathrm{PGA}}$ can be expressed as

$$\mu_{k\mathrm{PGA}} = \underbrace{\int_{-\infty}^{+\infty} \cdots \int_{-\infty}^{+\infty}}_{n} [\mathrm{PGA}(X_1, \cdots, X_i, \cdots, X_n)]^k \times f_{X_1}(x_1) \cdots f_{X_i}(x_i) \cdots f_{X_n}(x_n) dx_1 \cdots dx_i \cdots dx_n \cong \sum_{c=1}^{m} \prod_{i=1}^{n} W_{ci} [\mathrm{PGA}(X_{c1}, \cdots, X_{ci}, \cdots, X_{cn})]^k \tag{15}$$

where c is a combination of n items from a group $[1, 2, \cdots, m]$, m is the number of estimating points, ci is the ith term of c, and X_{ci} is the cith estimating point, W_{ci} is the weight corresponding to X_{ci}.

It should be noted that $\mu_{k\mathrm{PGA}}$ in Eq. (15) is dependent on the distribution of the random variable X_i. It is difficult to avoid that estimating points may move outside the region in which the random variable X_i are defined (Zhao and Ono 2000a). To avoid this problem, the estimating points were obtained in standard normal space (Zhao and Ono 2000a). By using the standard point estimate, Eq. (15) can be expressed as follows,

$$\mu_{k\mathrm{PGA}} = \underbrace{\int_{-\infty}^{+\infty} \cdots \int_{-\infty}^{+\infty}}_{n} [\mathrm{PGA}(X_1, \cdots, X_i, \cdots, X_n)]^k \times f_{X_1}(x_1) \cdots f_{X_i}(x_i) \cdots f_{X_n}(x_n) dx_1 \cdots dx_i \cdots dx_n = \underbrace{\int_{-\infty}^{+\infty} \cdots \int_{-\infty}^{+\infty}}_{n} \left[\mathrm{PGA}\left(T^{-1}(U_1, \cdots, U_i, \cdots, U_n)\right)\right]^k \times \phi_{U_1}(u_1) \cdots \phi_{U_i}(u_i) \cdots \phi_{U_n}(u_n) du_1 \cdots du_i \cdots du_n \cong \sum_{c=1}^{m} \prod_{i=1}^{n} W_{ci} \left[\mathrm{PGA}\left(T^{-1}(U_{c1}, \cdots, U_{ci}, \cdots, U_{cn})\right)\right]^k \tag{16}$$

where $X_i = T^{-1}(U_i)$ is the inverse normal transformation that can be realized by Rosenblatt transformation (Rackwitz and Flessler 1978) and third-moment transformation (Zhao and Ono 2000b), U_i is the ith standard normal random variable, U_{ci} is the cith estimating point in standard space, W_{ci} is the weight corresponding to U_{ci}, and $\varphi_{Ui}(u_i)$ is the PDF of U_i.

Because all distinct combinations must be considered, m^n function calls are required to calculate $\mu_{k\mathrm{PGA}}$. Therefore, the computations involved in Eq. (16) can be massive if n is large. Dimension-reduction integration (Xu and Rahman 2004) was adopted in this study to avoid this problem. Herein, to calculate the first three raw moments of the PGA, bivariate dimension reduction was used (Xu and Rahman 2004). The function $\mu_{k\mathrm{PGA}}$ can then be approximated using the following formula,

$$\mu_{k\mathrm{PGA}} \cong \sum_{1\le i<j\le n} I_2^k - (n-2)\sum_{i=1}^{n} I_1^k + \frac{(n-1)(n-2)}{2} I_0^k \tag{17}$$

where

$$\begin{aligned} I_0^k &= \left[\mathrm{PGA}\left(X_{1\mu},\cdots,X_{i\mu},\cdots,X_{n\mu}\right)\right]^k \\ I_1^k &= \int_{-\infty}^{+\infty}\left[\mathrm{PGA}\left(X_{1\mu},\cdots,T^{-1}(u_i),\cdots,X_{n\mu}\right)\right]^k f(x_i)dx_i \\ I_2^k &= \int_{-\infty}^{+\infty}\int_{-\infty}^{+\infty}\left[\mathrm{PGA}\left(X_{1\mu},\cdots,T^{-1}(u_i),\cdots,T^{-1}\left(u_j\right),\cdots,X_{n\mu}\right)\right]^k f(x_i)f\left(x_j\right)dx_i dx_j \end{aligned} \tag{18}$$

where $X_{i\mu}$ is the mean of the ith random variable X_i, I_0 is a function of all the variables based on their mean value, I_1 is a function of only u_i and $i = 1, 2, \cdots, n$, I_2 is a function of only u_i and u_j, $i, j = 1, 2, \cdots, n$, and $i < j$.

Using the point-estimate method in standard normal space, the one-dimensional integral ${I_1}^k$ in Eq. (18) can be estimated as follows,

$$I_1^k = \sum_{c=1}^{m} W_c\left[\mathrm{PGA}\left(X_{1\mu},\cdots,T^{-1}(u_{ci}),\cdots,X_{n\mu}\right)\right]^k \tag{19}$$

where u_{ci} is the cth estimating point of the ith standard normal random variable and W_c is the weight corresponding to u_{ci}.

Similarly, the two-dimensional integral ${I_2}^k$ in Eq. (18) can be estimated as

$$I_2^k = \sum_{c_1=1}^{m}\sum_{c_2=1}^{m} W_{c_1}W_{c_2}\left[\mathrm{PGA}\left(X_{1\mu},\cdots,T^{-1}(u_{ic_1}),\cdots,T^{-1}\left(u_{jc_2}\right),\cdots,X_{n\mu}\right)\right]^k \tag{20}$$

where c_1 is the estimating point of the first random variable in the function of u_i and u_j, c_2 is the estimating point of the second random variable in the function of u_i and u_j, u_{ic1} is the c_1th estimating point of u_i, u_{jc2} is the c_2th estimating point of u_j, W_{c1} is the weight corresponding to u_{ic1}, W_{c2} is the weight corresponding to u_{jc2}.

The detailed calculation flow of the proposed method is shown in Fig. 2. Equations (17–20) indicate that the proposed method needs to calculate PGA from FAS for $C_n^2 \times m^2 + C_n^1 \times m + 1$ times, as shown in Fig. 2. Considering 5 random variables and 7 estimating points (adopted in example 2, section 4), it only needs 526 calculations times of PGA from FAS when applying the proposed method, while for the same problem, the calculation time of PGA from FAS is usually larger than 10^5 when applying the method of Zhao, Zhang, and Zhang (2023), as shown in Fig. 1. The efficiency of the proposed method in calculating the exceedance probability of PGA is much better than the method of Zhao, Zhang, and Zhang (2023).

4. Numerical Examples and Investigations

To demonstrate the efficiency and accuracy of the proposed method, three examples are presented in this section: a point source, a plane source, and multiple plane sources. The three examples used the FAS model of the proposed method to calculate the exceedance probability of PGA. The mean values of the density of crust ρ, the stress drop $\Delta\sigma$, the shear-

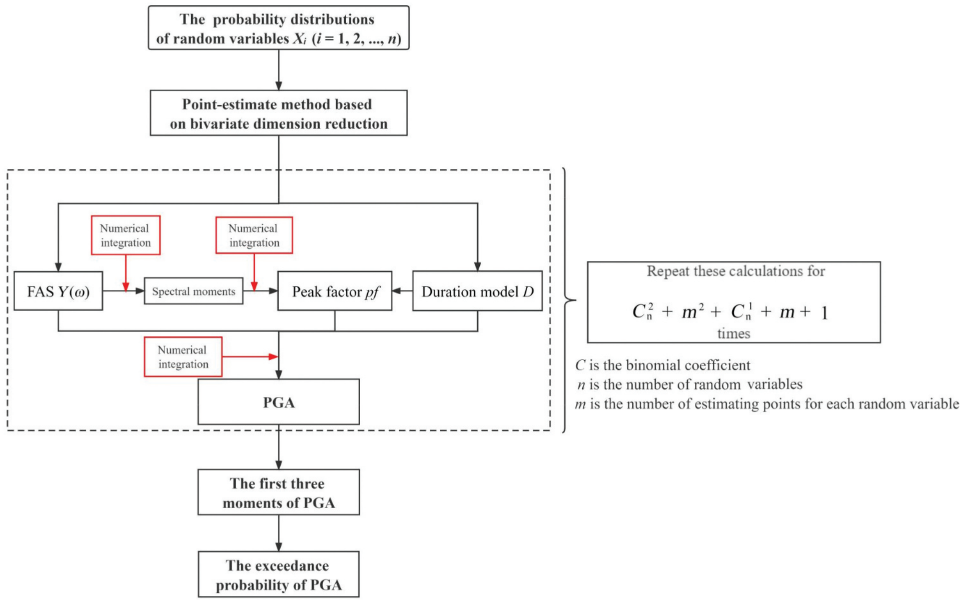

Figure 2. Flowchart of the proposed method.

Table 1. Probability distributions of the seismological parameters used in the Fourier amplitude spectral model.

Seismological parameters	Distribution	Mean	Standard deviation
Density of crust ρ (g/cm3)	Lognormal	2.8	0.56
Stress drop Δσ (bar)	Lognormal	400	100
Shear-wave velocity of crust β (km/s)	Lognormal	3.7	0.74
Site diminution κ0 (s)	Lognormal	0.04	0.012

Table 2. Other seismological parameters used in the Fourier amplitude spectral model.

Parameters	Value
Crust amplification A(f)	Boore and Thompson (2015)
Geometrical spreading Z(R)	Atkinson and Boore (2014)
Path attenuation	Atkinson and Boore (2014)

wave velocity of crust β, and site diminution κ_0 for East North America were adopted as listed in Table 1 (Zhang and Zhao 2020). The crust amplification $A(f)$, the geometrical spreading $Z(R)$, and the path attenuation for East North America were adopted as listed in Table 2 (Zhang and Zhao 2020). The expositions of the three examples are as follows.

4.1. Example 1. A Point Source

Example 1 considers a point source. The source-to-site distance R was 20 km. In addition, the average occurrence rate ν of the point source was assumed to be equal to 0.01 per year with $M \geq 6$. The time interval t was considered equal to 50 years. The truncated exponential recurrence model was used as the PDF of magnitude, where the minimum threshold magnitude m_{min} was six, the maximum threshold magnitude m_{max} was eight, and the statistical parameter θ was 2.6; this model can be expressed as

$$f_M(m) = \frac{2.6e^{-\theta m}}{e^{-\theta m_{\min}} - e^{-\theta m_{\max}}} \tag{21}$$

Folesky, Kummerow, and Shapiro (2021) pointed out that the probability distribution of stress drop $\Delta\sigma$ is a lognormal distribution. Although probability distributions of other seismological parameters, including the mass density of crust ρ, the shear-wave velocity of the crust β, and the diminution parameter κ_0 have received limited attention so far, it can easily infer that these parameters have uncertainties. More importantly, when these uncertainties are considered, the PGA varies even for a certain magnitude, distance, and site condition, which is consistent with real observation. This phenomenon (known as aleatory uncertainties) is commonly reflected using a sigma in the traditional GMPE of PGA. Thus, probability distributions of these parameters are all assumed to be lognormal distributions as listed in Table 1.

According to the probability distributions of the parameters in Table 1, the estimating points of κ_0, β, $\Delta\sigma$, and ρ can be obtained by Abramowitz and Stegun (1972). For a seven-point estimate ($m = 7$) in the standard normal space (Zhao and Ono 2000a), the estimating points and the corresponding weights are given by Eq. (22).

$$\begin{cases} u_{i_1} = -3.7504397 & w_1 = 5.48269 \times 10^{-4} \\ u_{i_2} = -2.3667594 & w_2 = 3.07571 \times 10^{-2} \\ u_{i_3} = -1.1544054 & w_3 = 0.2401233 \\ u_{i_4} = 0 & w_4 = 0.4571427 \\ u_{i_5} = 1.1544054 & w_5 = 0.2401233 \\ u_{i_6} = 2.3667594 & w_6 = 3.07571 \times 10^{-2} \\ u_{i_7} = 3.7504397 & w_7 = 5.48269 \times 10^{-4} \end{cases} \tag{22}$$

Using the proposed method, the conditional probability p_1 ($k = 1$ for one point source) in Eq. (10) can be obtained. For comparison, 100000 samplings were used in the MCS. The conditional probability that PGA exceeds *pga* given the occurrence of the 1st earthquake p_1 using the proposed method and the MCS are compared in Fig. 3.

Considering the average occurrence rate $v = 0.01$ per year with $M \geq 6$ and the time interval $t = 50$ years, the exceedance probability of PGA $P(\text{PGA} > pga; t)$ can be obtained. The calculations of $P(\text{PGA} > pga; \text{t})$ using the proposed method and the MCS are compared in Fig. 4.

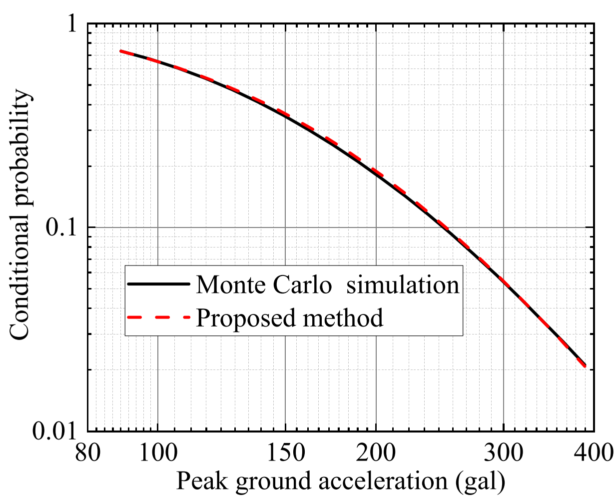

Figure 3. Conditional probability p_1 using the proposed method and the Monte Carlo simulations (MCS).

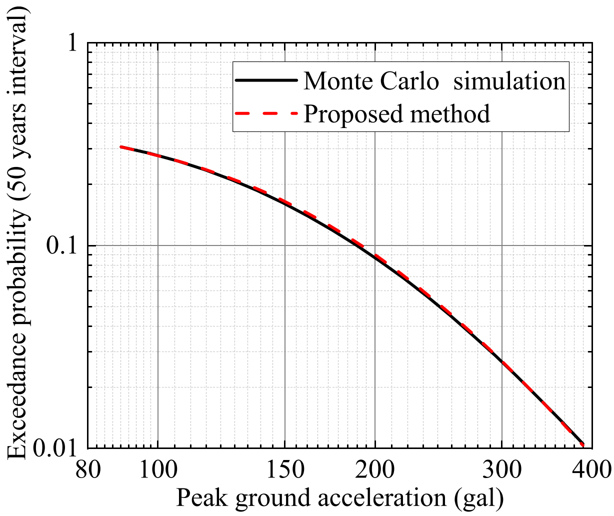

Figure 4. Exceedance probability of peak-ground acceleration (PGA) at 50 years intervals obtained using the proposed method and MCS with 1,000,000 samples.

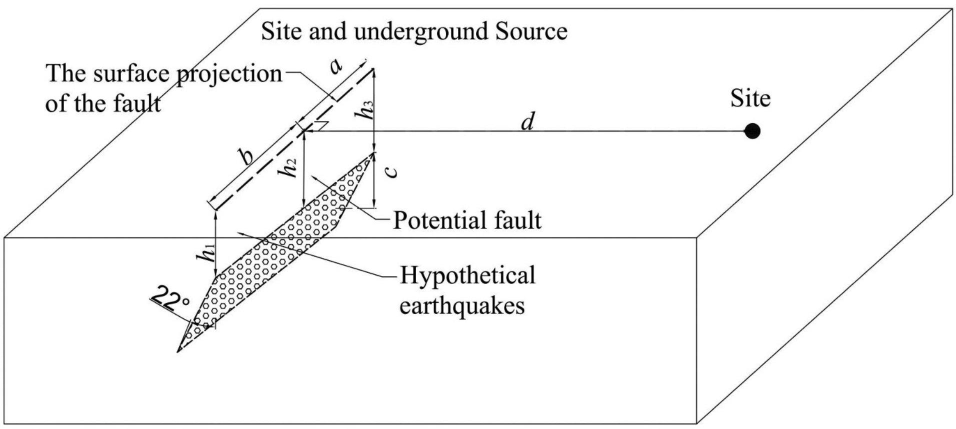

Figure 5. Example of a rectangular source; the circles represent hypothetical earthquakes.

As shown in Fig. 4, the results estimated by the proposed method are almost the same as those obtained by the MCS.

4.2. Example 2. A Plane Source

In this example, the plane source was rectangular ($500 \times 100\ \mathrm{km}^2$) and the minimum source-to-site distance was $d = 200$ km; and $a = 250$ km, $b = 350$ km, $c = 100$ km, the depth of hypocenter $h_1 = 10$ km, $h_2 = 12.9$ km, $h_3 = 15$ km, as shown in Fig. 5. The PDF of R can be obtained analytically according to the source geometry and relative location of the site by assuming that earthquakes have an equal likelihood of occurring anywhere in the plane source (Alamilla, Rodriguez, and Vai 2020). However, the obtained equations are excessively complex for practical application. To simplify the analysis, we adopted a lognormal distribution as an approximation for $f_R(r)$ according to Vetter and Taflanidis (2012) and Alamilla, Rodriguez,

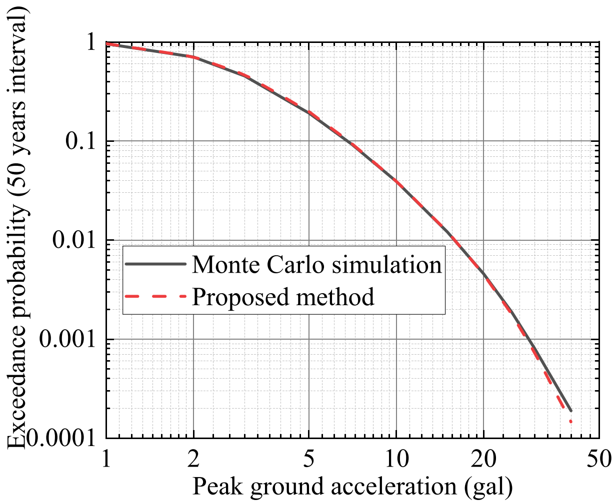

Figure 6. Exceedance probability of PGA at 50 years intervals obtained using the proposed method and using MCS with 100,000 samples.

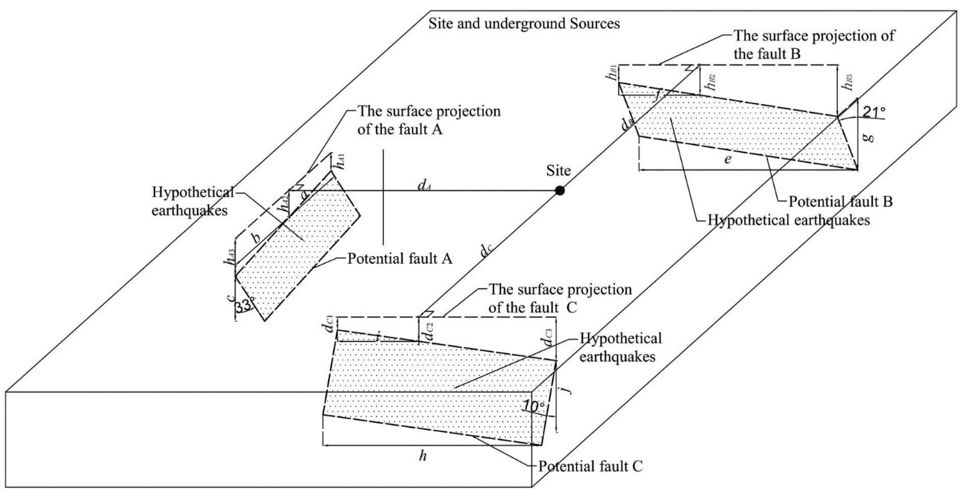

Figure 7. Distribution of the site and the seismic sources.

and Vai (2020). The mean value and standard deviation of distance R in $f_R(r)$ were determined as 233.33 km and 20.04 km, respectively, through MCS, assuming that earthquakes are equally probable across the entire plane source. The average occurrence rate v of the point source was assumed to be equal to 1 per year with $M \geq 6$. The truncated exponential recurrence model was used as the PDF of magnitude, where the minimum threshold magnitude m_{min} was six, the maximum threshold magnitude m_{max} was eight, the statistical parameter θ was 2.6. The time interval t was considered equal to 50 years.

The exceedance probability of PGA was obtained using an MCS with 1,000,000 samples and the proposed method. As shown in Fig. 6, the results estimated by the proposed method are almost the same as those obtained by MCS.

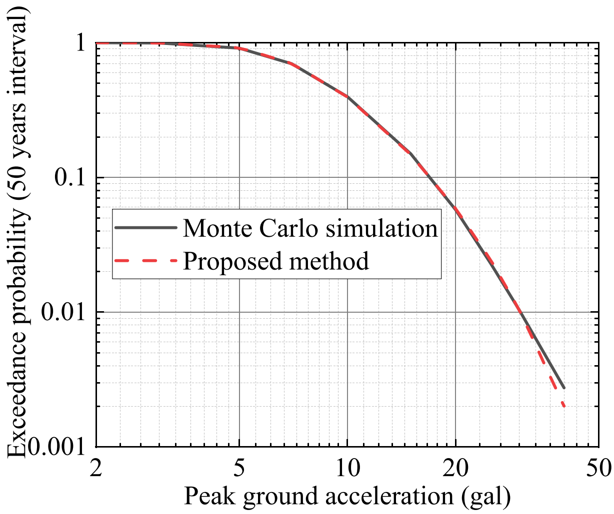

Figure 8. Exceedance probability of PGA at 50 years intervals obtained using the proposed method and MCS with 100,000 samples.

Table 3. Probabilistic distributions of the source-to-site distances in Example 3.

Source-to-site distance	Distribution	Mean (km)	Standard deviation (km)
R_A (for source *A*)	Lognormal	289.50	61.42
R_B (for source *B*)	Lognormal	282.43	24.22
R_C (for source *C*)	Lognormal	252.24	40.11

4.3. Example 3. Multiple Seismic Sources

The third example considers three plane sources, A, B, and C, as shown in Figure 7. For source A, the source-to-site minimum distance is $d_{\mathrm{A}} = 200$ km, and $a = 250$ km, $b = 350$ km, $c = 100$ km; the depth of hypocenter $h_{\mathrm{A}1} = 5$ km, $h_{\mathrm{A}2} = 7.9$ km, $h_{\mathrm{A}3} = 10$ km. For source B, the minimum source-to-site distance is $d_{\mathrm{B}} = 250$ km, and $e = 250$ km, $f = 100$ km, $g = 150$ km; the depth of hypocenter $h_{\mathrm{B}1} = 10$ km, $h_{\mathrm{B}2} = 13$ km, $h_{\mathrm{B}3} = 15$ km. For source C, the minimum source-to-site distance is $d_{\mathrm{C}} = 200$ km, and $h = 250$ km, $i = 50$ km, $j = 100$ km; $h_{\mathrm{C}1} = 10$ km, $h_{\mathrm{C}2} = 11$ km, $h_{\mathrm{C}3} =$ 15 km. The average occurrence rates of cases with $M \geq 6$ were $v_1 = 0.04$ for source A, $v_2 = 0.06$ for source B, and $v_3 = 0.12$ for source C. The truncated exponential recurrence model was used as the PDF of magnitude, where the minimum threshold magnitude m_{min} was six, the maximum threshold magnitude m_{max} was eight, the statistical parameter θ was 2.6 and the time interval t was 50 years.

The probability distributions of the uncertain seismological parameters are listed in Table 1, and the probability distributions of source-to-site distances are listed in Table 3. Other parameters of the FAS model are listed in Table 2. It was assumed that an earthquake occurred along a plane source with a uniform distribution.

The exceedance probability of PGA was obtained using an MCS with 1,000,000 samples and the proposed method. As shown in Figure 8, the results estimated by the proposed method are almost the same as those obtained by MCS.

For these three examples, it took as long as approximately 10 hours to complete the MCS considering 1,000,000 samples for each random variable. The proposed method required only 0.125 hours and provided nearly the same accuracy as MCS. From the discussion outlined above, it can be concluded that it is not only very efficient to obtain the exceedance probability of PGA by utilizing the proposed method, but also that the results estimated by the proposed method are almost the same as those obtained by the MCS method.

This study primarily focuses on the methodology for probability prediction of PGA. While the proposed approach offers many methodological advantages, as mentioned earlier, its practical implementation currently encounters challenges and requires further research in the future. Particularly, since there has been limited research on the probability distributions of some seismological parameters, this study makes certain assumptions. Future studies, similar to Folesky, Kummerow, and Shapiro (2021), exploring the probability properties of these seismological parameters, are expected to enhance the practical applicability of the proposed method.

5. Conclusion

This study presents an efficient method for the probabilistic prediction of PGA using FAS model based on the moment method. In contrast to the MCS, the moment method was introduced to simply calculate the exceedance probability of PGA in the proposed method. First, random vibration theory was used to obtain the PGA from the FAS. Second, the first three moments of PGA were obtained using the point-estimate method based on dimension reduction. Then, the exceedance probability of PGA could be estimated simply and accurately using a three-parameter probability distribution, in which the three parameters in the probability distribution were directly defined in terms of their first three moments. Three numerical examples were studied to demonstrate the accuracy and efficiency of the proposed evaluation method for the probabilistic prediction of PGA using the FAS model.

Acknowledgments

We gratefully acknowledge this support.

Disclosure Statement

No potential conflict of interest was reported by the author(s).

Funding

This study was partially supported by the National Natural Science Foundation of China [Grant Number 5227813].

Authors' Contributions

All authors contributed to the study conception and design. Data curation, writing-original draft preparation, visualization, conceptualization and methodology were performed by Rui Zhang, Yan-Gang Zhao and Haizhong Zhang. The first draft of the manuscript was written by Rui Zhang and all authors commented on previous versions of the manuscript. All authors read and approved the final manuscript.

Code Availability

Available upon request.

Data Availability Statement

All data generated or analyzed during this study are included in this published article. https://figshare.com/account/items/22578883/edit, DOI: 10.6084/m9.figshare.22578883.

References

Abramowitz, M. A., and I. A. Stegun. 1972. *Handbook of mathematical functions*, 924. New York: Dover. 10th Printing.

Alamilla, J. L., J. A. Rodriguez, and R. Vai. 2020. Unification of different approaches to probabilistic seismic hazard analysis. *Bulletin of the Seismological Society of America* 110 (6):2816–27. doi:10.1785/0120200148.

Atkinson, G. M. 1996. The high-frequency shape of the source spectrum for earthquakes in Eastern and Western Canada. *Bulletin of the Seismological Society of America* 86 (1A):106–12. doi:10.1785/BSSA08601A0106.

Atkinson, G. M. 2008. Ground-motion prediction equations for eastern north America from a referenced empirical approach: Implications for epistemic uncertainty. *Bulletin of the Seismological Society of America* 98 (3):1304–18. doi:10.1785/0120070199.

Atkinson, G. M., and D. M. Boore. 2006. Earthquake ground-motion prediction equations for Eastern North America. *Bulletin of the Seismological Society of America* 96 (6):2181–205. doi:10.1785/0120050245.

Atkinson, G. M., and D. M. Boore. 2014. The attenuation of Fourier amplitudes for rock sites in Eastern North America. *Bulletin of the Seismological Society of America* 104 (1):513–28. doi:10.1785/0120130136.

Atkinson, G. M., and W. Silva. 2000. Stochastic modeling of California ground motions. *Bulletin of the Seismological Society of America* 90 (2):255–74. doi:10.1785/0119990064.

Boore, D. M. 1983. Stochastic simulation of high-frequency ground motions based on seismological models of the radiated spectra. *Bulletin of the Seismological Society of America* 73 (6A):1865–94.

Boore, D. M. 2003. Simulation of ground motion using the stochastic method. *Pure and Applied Geophysics* 160 (3):635–76. doi:10.1007/PL00012553.

Boore, D. M. 2018. Ground motion models for very-hard-rock sites in Eastern North America: An update. *Seismological Research Letters* 89 (3):1172–84. doi:10.1785/0220170218.

Boore, D. M. 2020. Revision of Boore (2018) ground-motion predictions for central and Eastern North America: Path and offset adjustments and extension to 200 m/s ≤ VS30 ≤ 3000 m/s. *Seismological Research Letters* 91 (2A):977–91. doi:10.1785/0220190190.

Boore, D. M., and W. B. Joyner. 1997. Site amplifications for generic rock sites. *Bulletin of the Seismological Society of America* 87 (2):327–41. doi:10.1785/BSSA0870020327.

Boore, D. M., and E. M. Thompson. 2015. Revisions to some parameters used in stochastic-method simulations of ground motion. *Bulletin of the Seismological Society of America* 105 (2A):1029–41. doi:10.1785/0120140281.

Bora, S. S., F. Cotton, and F. Scherbaum. 2019. NGA-West2 empirical Fourier and duration models to generate adjustable response spectra. *Earthquake Spectra* 35 (1):61–93. doi:10.1193/110317EQS228M.

Bora, S. S., F. Scherbaum, N. Kuehn, and P. Stafford. 2014. Fourier spectral- and duration models for the generation of response spectra adjustable to different source-, propagation-, and site conditions. *Bulletin of Earthquake Engineering* 12 (1):467–93. doi:10.1007/s10518-013-9482-z.

Bora, S. S., F. Scherbaum, N. Kuehn, and P. Stafford. 2016. On the relationship between Fourier and response spectra: Implications for the adjustment of empirical ground-motion prediction equations (GMPEs). *Bulletin of the Seismological Society of America* 106 (3):1235–53. doi:10.1785/0120150129.

Bora, S. S., F. Scherbaum, N. Kuehn, P. Staford, and B. Edwards. 2015. Development of a response spectral ground-motion prediction equation (GMPE) for seismic-hazard analysis from empirical Fourier spectral and duration models. *Bulletin of the Seismological Society of America* 105 (4):2192–218. doi:10.1785/0120140297.

Campbell, K. W. 2003. Prediction of strong ground motion using the hybrid empirical method and its use in the development of ground-motion (attenuation) relations in Eastern North America. *Bulletin of the Seismological Society of America* 93 (3):1012–33. doi:10.1785/0120020002.

Campbell, K. W. 2009. Estimates of shear-wave Q and κ_0 for unconsolidated and semiconsolidated sediments in Eastern North America. *Bulletin of the Seismological Society of America* 99 (4):2365–92. doi:10.1785/0120080116.

Cartwright, D. E., and M. S. Longuet-Higgins. 1956. The statistical distribution of the maxima of a random function. *Proceedings of the Royal Society of London. Series A, Mathematical and Physical Sciences* 237: 212–32.

Cornell, C. A. 1968. Engineering seismic risk analysis. *Bulletin of the Seismological Society of America* 58 (5):1583–606. doi:10.1785/BSSA0580051583.

Cotton, F., F. Scherbaum, J. J. Bommer, and H. Bungum. 2006. Criteria for selecting and adjusting ground-motion models for specific target regions: Application to central Europe and rock sites. *Journal of Seismology* 10 (2):137. doi:10.1007/s10950-005-9006-7.

Davenport, A. G. 1964. Note on the distribution of the largest value of a random function with applications to rust loading. *Proceedings of the Institution of Civil Engineers* 28 (2):187–96. doi:10.1680/iicep.1964.10112.

Douglas, J. 2021. Ground motion prediction equations 1964–2021. http://www.gmpe.org.uk/.

Drouet, S., G. Ameri, K. L. Dortz, R. Secanell, and G. Senfaute. 2020. A probabilistic seismic hazard map for the metropolitan France. *Bulletin of Earthquake Engineering* 18 (5):1865–98. doi:10.1007/s10518-020-00790-7.

Du, W. Q., and T. C. Pan. 2020. Probabilistic seismic hazard assessment for Singapore. *Natural Hazards* 103 (3):2883–903. doi:10.1007/s11069-020-04107-4.

Eurocode 8. 2004. *Design of structures for earthquake resistance, part 1: General rules, seismic actions and rules for buildings*. EN 2004–1–1. Brussels, Belgium: European Committee for Standardization (CEN).

Falak, Z., A. Abdullah, R. K. Seshagiri, and N. Satyam. 2023. Seismic hazard assessment of Kashmir Region using logic tree approach: Focus on sensitivity of PSHA results towards declustering procedures and GMPEs. *Pure and Applied Geophysics* 180 (3):789–827. doi:10.1007/s00024-023-03239-5.

Folesky, J., J. Kummerow, and S. A. Shapiro. 2021. Stress drop variations in the region of the 2014 M_W8.1 Iquique Earthquake, Northern Chile. *Journal of Geophysical Research* 126 (4):1–20. doi:10.1029/2020jg005684.

Foytong, P., T. Ornthammarathb, R. Arjwech, A. Janpila, N. Areemit, A. Ruangrassamee, and P. Chindaprasirt. 2020. Probabilistic seismic hazard assessment of North-Eastern Thailand. *Journal of Civil Engineering* 24 (4):1–13.

Fujiwara, H., S. Kawai, S. Aoi, N. Morikawa, S. Senna, K. Kobayashi, T. Ishii, T. Okumura, and Y. Hayakawa. 2006. National seismic hazard maps for Japan. *Bulletin of Earthquake Research Institute* 81:221–32.

GB 18306-2015. 2015. *Seismic ground motion parameters zonation map of China*. Beijing: China Building Industry Press. (In Chinese).

GB 50011-2010. 2016. *Code for seismic design of buildings*, 2016 ed. Beijing: China Building Industry Press. (In Chinese).

Hanks, T. C. 1979. *B* values and ω-γ seismic source models: Implications for tectonic stress variations along active crustal fault zones and the estimation of high-frequency strong ground motion. *Journal of Geophysical Research* 84 (B5):2235–42. doi:10.1029/JB084iB05p02235.

Hanks, T. C., and H. Kanamori. 1979. A moment magnitude scale. *Journal of Geophysical Research* 84 (B5):2348–50. doi:10.1029/JB084iB05p02348.

Hanks, T. C., and R. K. McGuire. 1981. The character of high-frequency strong ground motion. *Bulletin of the Seismological Society of America* 71 (6):2071–95. doi:10.1785/BSSA0710062071.

Hassani, B., and G. M. Atkinson. 2015. Referenced empirical ground-motion model for Eastern North America. *Seismological Research Letters* 86 (2):477–91.

Hsu, T. Y., R. T. Wu, C. W. Liang, C.-H. Kuo, and C.-M. Lin. 2020. Peak ground acceleration estimation using P-wave parameters and horizontal-to-vertical spectral ratios. *Terrestrial Atmospheric and Oceanic Sciences* 31 (1):1–8. doi:10.3319/TAO.2019.07.04.01.

Jarahi, H. 2017. PSHA study using EZ-Frisk software case study Baychebaq Dam Site. *Current Research in Geosciences* 7 (2):37–46. doi:10.3844/ajgsp.2017.37.46.

JGJ 3-2010. 2010. *Technical specification for concrete structures of tall building*. Beijing: China Building Industry Press. (In Chinese).

Kolli, M. K., and S. S. Bora. 2021. On the use of duration in random vibration theory (RVT) based ground motion prediction: A comparative study. *Bulletin of Earthquake Engineering* 19 (4):1687–707. doi:10.1007/s10518-021-01052-w.

Kottke, A. R., and E. M. Rathje. 2013. Comparison of time series and random-vibration theory site-response methods. *Bulletin of the Seismological Society of America* 103 (3):2111–27. doi:10.1785/0120120254.

Li, B., M. B. Sørensen, K. Kuvvet Atakan, Y. Li, and Z. Li. 2020. Probabilistic seismic hazard assessment for the Shanxi Rift system, North China. *Bulletin of the Seismological Society of America* 110 (1):127–53. doi:10.1785/0120190099.

Mahmoud, E., S. A. Mohamed, and G. Hanan. 2021. Up-to-date PSHA along the Gulf of Aqaba-Dead Sea transform fault. *Soil Dynamics and Earthquake Engineering* 148 (4):106835. doi:10.1016/j.soildyn.2021.106835.

McGuire, R. K. 1976. "FORTRAN computer program for seismic risk analysis," United States department of the interior geological survey. Open-File Report, 76–67.

Nakano, K., and H. Kawase. 2019. Source parameters and site amplifications estimated by generalized inversion technique: Focusing on the 2018 Hokkaido Iburi-Tobu earthquake. *Earth, Planets and Space* 71 (1):66. doi:10.1186/s40623-019-1047-1.

Rackwitz, R., and B. Flessler. 1978. Structural reliability under combined random load sequences. *Computers & Structures* 9 (5):489–94. doi:10.1016/0045-7949(78)90046-9.

Rahman, A., F. A. Najam, S. Zaman, A. Rasheed, and I. A. Rana. 2021. An updated probabilistic seismic hazard assessment (PSHA) for Pakistan. *Bulletin of Earthquake Engineering* 19 (4):1625–62. doi:10.1007/s10518-021-01054-8.

Rathje, E. M., and M. C. Ozbey. 2006. Site-specific validation of random vibration theory-based seismic site response analysis. *Journal of Geotechnical and Geoenvironmental Engineering* 132 (7):911–22. doi:10.1061/(ASCE)1090-0241(2006)132:7(911).

RLB. 2015. *Recommendations for loads on buildings*. Tokyo: Architectural Institute of Japan. (in Japanese).

Rosenblueth, E. 1975. Point estimates for probability moments. *Proceedings of the National Academy of Sciences of the United States of America* 72 (10):3812–14. doi:10.1073/pnas.72.10.3812.

Saurav, S., S. Aniruddha, H. Reginald, J. Dehls, R. K. Bhasin, I. Penna, and V. Gupta. 2022. Probabilistic seismic hazard analysis (PSHA) to estimate the input ground motions for co-seismic landslide hazard assessment: A case study on Himalayan highways, Sikkim India. *Physics and Chemistry of the Earth* 127:103157. doi:10.1016/j.pce.2022.103157.

Sinhal, R., and R. Sarkar. 2020. Seismic hazard assessment of Dhanbad City, India, by deterministic approach. *Natural Hazards* 103 (2):1857–80. doi:10.1007/s11069-020-04059-9.

Sun, X. D., X. X. Tao, S. S. Duan, and C. Liu. 2013. Kappa (κ) derived from accelerograms recorded in the 2008 Wenchuan, mainshock, Sichuan, China. *Journal of Asian Earth Sciences* 73:306–16. doi:10.1016/j.jseaes.2013.05.008.

Vanmarcke, E. H. 1975. On the distribution of the first-passage time for normal stationary random processes. *Journal of Applied Mechanics* 42 (1):215–20. doi:10.1115/1.3423521.

Vanmarcke, E. H., and S. S. P. Lai. 1980. Strong-motion duration and RMS amplitude of earthquake records. *Bulletin of the Seismological Society of America* 70 (4):1293–307.

Vetter, C., and A. A. Taflanidis. 2012. Global sensitivity analysis for stochastic ground motion modeling in seismic-risk assessment. *Soil Dynamics and Earthquake Engineering* 38:128–43. doi:10.1016/j.soildyn.2012.01.004.

Villani, M., Z. Lubkowski, M. Free, R. M. W. Musson, B. Polidoro, R. McCully, A. Koskosidi, C. Oakman, T. Courtney, M. Walsh, et al. 2020. A probabilistic seismic hazard assessment for Wylfa Newydd, a new nuclear site in the United Kingdom. *Bulletin of Earthquake Engineering* 18 (9):4061–89. doi:10.1007/s10518-020-00862-8.

Wang, X., and E. M. Rathje. 2016. Influence of peak factors on site amplification from random vibration theory based site-response analysis. *Bulletin of the Seismological Society of America* 106 (4):1–14. doi:10.1785/0120150328.

Wang, X., and E. M. Rathje. 2018. Development of ground-motion duration models for use in random vibration theory site-response analysis. *Bulletin of the Seismological Society of America* 108 (4):2104–16. doi:10.1785/0120170211.

Xu, H., and S. Rahman. 2004. A generalized dimension-reduction method for multi-dimensional integration in stochastic mechanics. *International Journal for Numerical Methods in Engineering* 61 (12):1992–2019. doi:10.1002/nme.1135.

Zhang, H. Z., and Y. G. Zhao. 2020. Damping modification factor based on random vibration theory using a source-based ground-motion model. *Soil Dynamics and Earthquake Engineering* 136:106225. doi:10.1016/j.soildyn.2020.106225.

Zhao, Y. G., and Z. H. Lu. 2021. *Structural reliability: Approaches from perspectives of statistical moments*. 1st ed. Hoboken: Wiley.

Zhao, Y. G., and T. Ono. 2000a. New point-estimates for probability moments. *Journal of Engineering Mechanics* 126 (4):433–36. doi:10.1061/(ASCE)0733-9399(2000)126:4(433).

Zhao, Y. G., and T. Ono. 2000b. Third-moment standardization for structural reliability analysis. *Journal of Structural Engineering* 126 (6):724–32. doi:10.1061/(ASCE)0733-9445(2000)126:6(724).

Zhao, Y. G., T. Ono, H. Idota, and T. Hirano. 2001. A three-parameter distribution used for structural reliability evaluation. *Journal of Structural & Construction Engineering* 66 (546):31–38. doi:10.3130/aijs.66.31_6.

Zhao, Y. G., R. Zhang, and H. Z. Zhang. 2023. Probabilistic prediction of ground-motion intensity for regions lacking strong ground-motion records. *Soil Dynamics and Earthquake Engineering* 165:107706. doi:10.1016/j.soildyn.2022.107706.